JOURNAL OF MATERIALS SCIENCE 32 (1997) 5661–5667

Morphology of a deformed rubber toughened poly(methyl methacrylate) film under tensile strain

C. HE, A. M. DONALD*
Polymer and Colloids Group, Cavendish Laboratory, University of Cambridge, Cambridge, CB3 0HE, UK

The morphology of rubber toughened poly(methyl methacrylate) (PMMA) films was studied during deformation using environmental scanning electron microscopy (ESEM) combined with real time small angle X-ray scattering (SAXS). These two methods provide two different approaches to an *in situ* study of the morphology of the deforming polymer film. The ESEM study shows that the polymer film exhibits multiple craze-like streaks under tensile strain. Every streak runs through several apparently cavitated rubber particles. Further study by SAXS reveals that these streaks are not crazes. Instead they appear to be lines of cavitated rubber particles which form a particular type of dilatation band known as a ''croid''. The ESEM study also shows that with increasing strain the rubber particles gradually increase in size, and that both the number and size of the croids increase. Finally the croids evolve into cracks just before the breakdown of the sample.

1. Introduction

Rubber toughening of polymers is a frequently used strategy to improve the toughness of thermoplastic polymers, since rubber particles can act as cavitation centres and crazing nuclei, processes which can dissipate energy during fracture hence resulting in a better toughness [1]. In order to understand the underlying failure mechanisms and hence to design an effective strategy to improve their mechanical properties, the morphologies of deformed polymer matrices have been extensively studied [2–4, 5–7]. The deformation mechanisms of polymers can be classified into two major types: crazing and non-crazing (including shear yield and cavitation) which have their own characteristics, and which can directly determine the failure mechanism.

The imaging methods employed in these earlier studies were mainly transmission and scanning electron microscopy (TEM and SEM respectively). However, TEM and SEM studies require a high vacuum environment allied to coated samples. The structures observed can only be considered as arising from a post mortem analysis, with the possibility of some artefacts having been introduced into the observed morphologies. When *in situ* deformation has been carried out in an SEM, charging problems due to the opening up of fresh, uncoated surfaces inevitably arise [8]. ESEM is a modified version of a conventional SEM [9]. A differential pumping system and a different type of detector [10] not only allows the specimen chamber to contain water vapour during imaging, but also allows insulating samples to be examined without coating. These advantages added to the utilization of a small tensile rig, make ESEM well suited for an *in situ* real time study of the changing morphologies which form during polymer deformation, of a type unachievable using conventional SEM or TEM. This is particularly useful since deformed or cavitated rubber particles may change their structures when the applied stress is removed. As a result, the post mortem analysis by TEM and SEM may fail to reveal the true structure of rubber particles during deformation. The alternative technique of real time small angle X-ray scattering (SAXS) has also been increasingly used for the study of rubber toughened systems during *in situ* deformation [11, 12]. It provides a complementary method to an understanding of the morphologies observed in ESEM. This paper reports results on the structures that form upon deformation of thin rubber toughened poly(methyl methacrylate) films determined using a combination of ESEM imaging and SAXS analysis. This particular combination is very powerful since it combines the direct image of small regions of the film seen in the ESEM with the spatially averaged information obtained from scattering methods.

2. Experimental procedures

The polymer film was supplied by ICI plc. It contains about 40 wt % of core-shell rubber particles. The core-

* To whom correspondence should be addressed.

0022–2461 © *1997 Chapman & Hall*

shell rubber particle consists of a three-layer structure: a PMMA core, a rubber middle layer and an outer PMMA layer. The PMMA core has a diameter of 150 nm. The middle rubber layer has a thickness of 40 nm and there is a very thin outer PMMA layer, which ensures good adhesion with the surrounding PMMA matrix. The crosslinking level of the rubber layer is 2%. The thickness of the film is about 100 μm. For the ESEM study the polymer film was cut into a rectangle, 30 × 8 mm in size. For the SAXS study, the sample was cut into a shape described previously [11] for the study of thick samples; the shape is designed to ensure that the X-ray beam passes through the deforming region of the sample during deformation. The irregular shape of the SAXS sample makes it difficult to obtain the true strain so that the result cannot be quantitatively compared with the ESEM analysis. Nevertheless, the evolution of the deformation can easily be studied by SAXS analysis, and in turn this helps us to understand in more detail the morphologies observed in the ESEM study. Additionally, since the ESEM is necessarily only able to observe the surface of the film whereas the SAXS results correspond to a volume of sample, a check is placed on the validity of the ESEM approach.

The films were mounted in a tensile rig which was then fitted into the ESEM sample stage. The ESEM used was an Electroscan E3 model. The pump down sequence described by Cameron and Donald [13] was followed, to ensure proper conditions for imaging. After suitable imaging conditions were established, the sample was drawn to a certain strain and then viewed. The effective length of the polymer sample subjected to strain is about 11 mm. The extension rate is 50 μm s^{-1}. Care needs to be taken to minimize beam damage by limiting exposure time (or increasing the scanning rate). In practice, focusing was carried out in one region and then the beam moved to another fresh (unexposed) region before a micrograph was taken. This minimizes the beam damage in the micrographs.

The SAXS experiment was carried out at the Daresbury synchrotron radiation source on station 2.1 using a 2-D multiwire proportional gas filled area detector. A miniature materials testing rig ("Minimat" from Polymer Laboratories) was fitted into the beam line. The sample was subjected to tensile strain and the tensile curve and the SAXS pattern were simultaneously recorded. The frame time used was about 8 s, and every sample has 30–50 frames of data. The sample to detector distance is 600 mm. The tensile axis in this experiment is vertical. The strain rate is 0.5 mm min^{-1}. Due to the irregular shape of the sample, the true strain rate of the sample sampled by the X-ray is difficult to determine. A more detailed account of the experimental set up and data analysis will be given in a future paper [14].

3. Results

3.1. ESEM study

Fig. 1 is an ESEM micrograph of an undeformed (and uncoated) polymer film, which shows a featureless surface. As tensile strain is applied, the rubber particles become visible, and many streaks appear in the surface. Fig. 2a shows the structure when the total extension has reached 2.5 mm (engineering strain of 22.7%), in which these streaks – running between rubber particles – are clearly visible in the surface of the film. The striking feature is that these streaks run normal to the tensile axis. It is worth noting that the initially transparent polymer film has become opaque by this stage. Fig. 2b is a higher magnification view of part of Fig. 2a. As the strain increases so does the

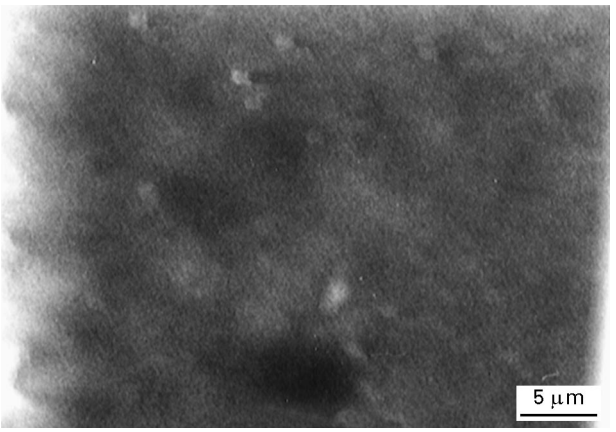

Figure 1 ESEM micrograph of undeformed polymer film, showing a featureless morphology.

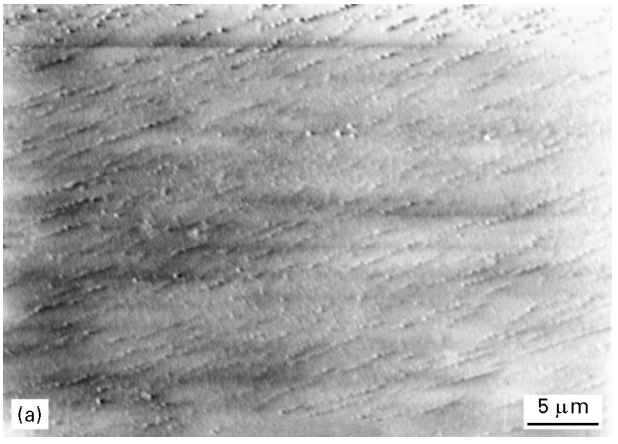

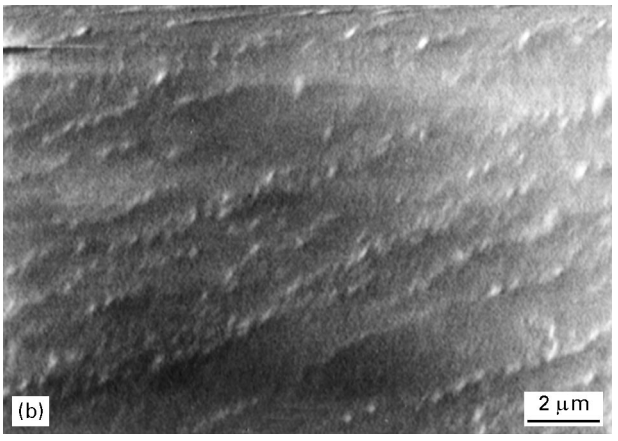

Figure 2 (a) ESEM micrograph of deformed polymer film. Total extension is about 2.5 mm. The rubber particles have become visible and there are some streaks running normal to the tensile axis. (b) Magnified view of part of (a).

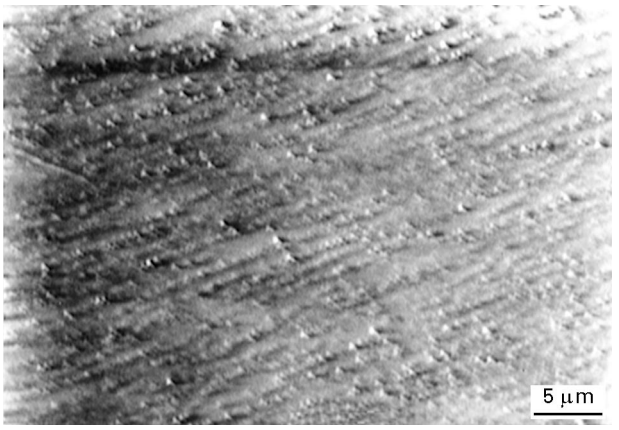

Figure 3 ESEM micrograph of a deformed film, at an extension of 4.2 mm. The population and size of streaks has increased compared with Fig. 2a.

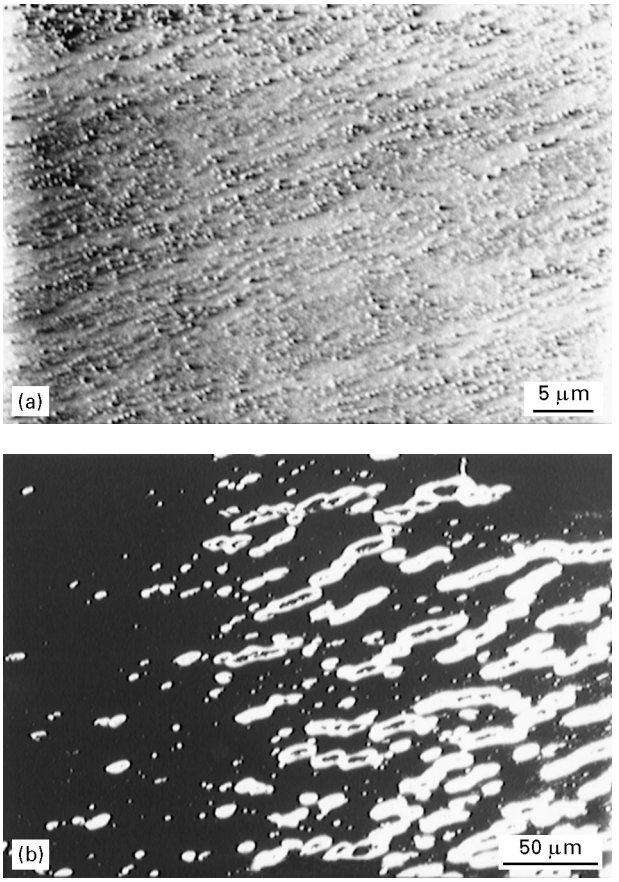

Figure 4 (a) ESEM micrograph of a deformed film at an extension of 7 mm. The population and size of streaks has increased further and the streaks become brighter. (b) ESEM micrograph of a deformed film at an extension of 7 mm, showing a region in which significant cracking has now occurred.

density of these streaks, and concurrently the visibility of the rubber particle also increases. Fig. 3 shows the structure at an extension of 4.2 mm (engineering strain of 38.2%). By an extension of 7 mm (engineering strain of 63.6%) which is just before the final breakdown of the polymer film (at about 8 mm), the number density of these streaks and their size (width and length) has increased significantly, as is shown in Fig. 4a. (Note that the distribution of rubber particles in the polymer matrix is quite homogeneous as can be seen from the micrograph). Moreover, large cracks also appear at this stage of deformation as shown in Fig. 4b. These cracks are so big that they adsorb a larger amount of condensed water than the rest of the film and this gives rise to bright contrast at the edge of a crack (the origin of bright contrast due to localization of water is discussed in reference [15]). An additional point to be noted relates to the rubber particles themselves. They appear to increase in size as the strain increases, as can be seen by comparing Figs 2a and 3. Although Fig. 2a has a slightly higher magnification, the particle sizes appear to be smaller than in Fig. 3.

3.2. Small angle X-ray study

For an undeformed film, the SAXS pattern looks like an ellipse as is shown in Fig. 5a. This is the standard form of SAXS pattern from such a system, and contains the signature of the form factor of the particle [11], although most of the detail of this is obscured by the beam stop. The ellipsoidal shape indicates that the rubber particles already possess some level of orientation, arising from the processing history of the film; the film has been extruded and drawn, so providing an initial orientation of the rubber particles. For this SAXS experiment, the initial orientation of the rubber lies parallel to the tensile axis. Fig. 5b is a 2-D SAXS pattern of the sample deformed to an extension of 2.7 mm (due to the irregular shape, the true strain of the sample is difficult to attain). The scattering pattern changes from an ellipse to a shape approximating to a diamond. As the sample is stretched further, the scattering pattern moves in to a lower angle, as is shown in Fig. 5c in which the total extension is

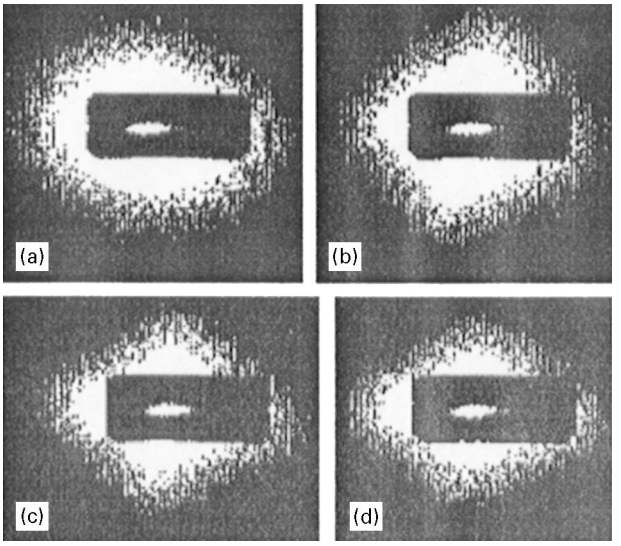

Figure 5 (a) 2-D small angle X-ray scattering of undeformed polymer film. The elliptical scattering indicates rubber particles in the polymer matrix are already oriented due to the processing history. (b) 2-D small angle X-ray scattering of deformed polymer film at an extension of 2.7 mm. (c) 2-D small angle X-ray scattering of deformed polymer film at an extension of 5.4 mm. (d) 2-D small angle X-ray scattering of deformed polymer film at an extension of 6.1 mm.

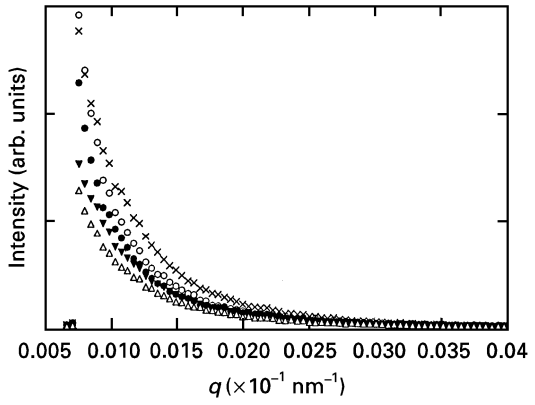

Figure 6 1-D small angle X-ray scattering curve presenting the meridional scattering from the 2-D pattern. The key to the number of the data frame, with extension is; (○) frame 1: 0 mm; (●) frame 10: 1.35 mm; (×) frame 20: 2.7 mm; (▼) frame 40: 5.4 mm and (△) frame 45: 6.1 mm. $q = 4\pi \sin\theta/\lambda$.

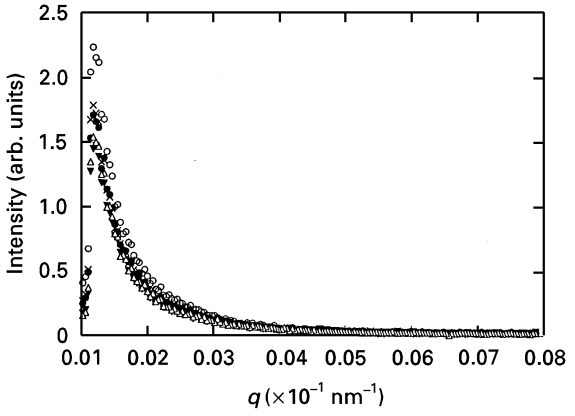

Figure 7 1-D small angle X-ray scattering curve representing the equatorial scattering from the 2-D pattern. The key to the number of the data frame, with extension is; (○) frame 1: 0 mm; (×) frame 10: 1.35 mm; (●) frame 20: 2.7 mm; (▼) frame 40: 5.4 mm and (△) frame 45: 6.1 mm. $q = 4\pi \sin\theta/\lambda$.

5.4 mm. In the final stage of deformation, but before the sample broke, the scattering pattern shrank further. Fig. 5d shows the X-ray scattering at this stage where the total extension was about 6.1 mm.

Looking at the meridional scattering alone as shown in Fig. 6, it can be seen that during the early stages of deformation (frame 1 to frame 10) the scattering intensity moves to a lower angle with increasing strain. As the strain increases further, the scattering then moves out to higher angle, as shown for frame 20. After that, the scattering moves to a lower angle again as the strain continues to increase, as shown for frames 40 and 45. However, for the equatorial scattering, the intensity of scattering shows little change during the entire process of deformation, as shown in Fig. 7.

4. Discussion

4.1. Characteristics of "streaks"

The dominant feature seen in the ESEM following tensile straining is the appearance of many "streaks" on the surface of the sample, in contrast to the undeformed sample whose surface is featureless, as shown in Fig. 1. As the deformation progresses, the rubber particles become more visible. Furthermore, these streaks appear normal to the tensile axis. In that sense they are reminiscent of crazes which usually grow in this direction. However it does not necessarily follow that these features are indeed crazes.

In order to address this question, more detailed information regarding the internal structure of the streaks is required, which can be obtained from the real time SAXS experiment. If crazes are the only source of low angle scattering, a "cross" will be seen in the scattering pattern [16]. Using the same geometry as in this study, i.e., with the tensile axis vertical, the meridional scattering represents the scattering from the craze interfaces, while the equatorial scattering is due to scattering from fibrils within the crazes [16]. However, since core–shell rubber particles are used in this polymer system, there is additionally scattering along both the meridian and equatorial arising from the form factor of the rubber particles. Although this complicates the scattering pattern, it is possible to separate out the two contributions so that the crazing can be quantitatively analysed [11, 17].

Within this well-established framework, it is possible to deduce the changes in the sample during deformation and compare them with the morphologies observed in the ESEM. Since craze fibrils can be quantitatively related to the scattering on the equator [16], a conclusive test of whether crazes are forming comes from examination of the equatorial scattering. If the streaks seen in the ESEM are crazes, then there should be an increased scattering from the fibrils on the equator of the scattering pattern. Fig. 7 showed the results for the scattering intensity along the equator as deformation proceeds. It can be seen that the intensity of the equatorial scattering hardly changes at all during the course of deformation, suggesting that either there is no crazing in the polymer film or that the craze density is so low that it is below the resolution of the SAXS analysis. Hence, these craze-like streaks are not in fact due to crazing at all, but from some other sort of structure.

Recent studies [2, 3] have shown that there is another possibility which could lead to an appearance of streaks normal to the tensile axis. A TEM study of core–shell rubber modified epoxy [2] showed that the crack tip damage zones of the matrix appear to consist of multiple lines of craze-like damage and massive shear banding. The damage zone was found to be a collection of cavitated particles lying ahead of an advancing crack and was termed a "croid". It was regarded as being "craze-like" in that the croids show up as lines which are normal to the tensile axis. Lazzeri and Bucknall suggested that "croids" can be regarded as a particular type of dilatation band which could appear in toughened polymer matrices particularly when the distribution of rubber particle size is narrow [3, 4]. This is because if the particle size distribution is narrow, all the particles tend to cavitate simultaneously. As a result, the effective volume fraction of voids is high within a given small zone, and the angle, ψ, (which the normal to the dilatation band

makes with the tensile axis) is therefore close to zero leading to the "croids" being normal to the tensile axis.

Previous studies by SAXS on these same core–shell particles' internal morphologies [11, 14] and by ESEM on the particles' sizes [18] have shown that the size distribution of the core–shell particles is indeed narrow which, by the above argument, would favour the formation a dilatation band normal to the tensile axis. In addition, it is well known that deformation bands are more prone to lie normal to the tensile axis for thin films [19]. All these results indicate that the streaks observed in our study are a particular type of dilatation band arising from lined up cavitated rubber particles. The ESEM study cannot conclusively reveal if there is shear banding between the particles, but the micrographs are suggestive of deformation between the particles as well as cavitation of the particles themselves.

4.2. Morphology of polymer film during deformation

Having understood the nature of the streaks, we can now examine their structural evolution during the course of deformation. Firstly, in Figs 1–4(a and b) it can be seen that there is a progressive increase in the population and size of croids as the strain increases, indicating that the plastic deformation of the film is mainly due to localized voiding (cavitation and/or debonding) of rubber particles which induces these micro dilatation bands. Secondly, the size of the rubber particle increases gradually as the strain increases. It can be seen that the size of the visible (i.e., presumed cavitated) rubber particles in Fig. 3 are about twice that in Fig. 2a. There are two possible ways to explain this changing particle size. One possibility follows Sue's [2] result that in the damage zone all the rubber particles are fully cavitated (or debonded). If this is the case, what we see in the micrographs is due to expansion of the fully cavitated (or debonded) rubber particles as the strain increases. The other possibility is that in the damage zone, the rubber particles have not yet fully cavitated or debonded but they undergo a progressive evolution of voiding (cavitation or debonding). As a result, the particle size grows gradually as seen in the micrograph. At the present moment we cannot distinguish which mechanism is occurring.

Such a gradual evolution in particle size could not be seen from a post mortem analysis using TEM or SEM methods, particularly since there is the possibility of recovery once the tensile stress is removed. By contrast, in the ESEM, the sample is imaged during the course of deformation and hence this expansion can be followed. This is an advantage of using ESEM for such studies, although it must be remembered that it can only image the surface of the sample.

A further confirmation of the appearance of voiding (cavitation or debonding) in the matrix comes from the study of the meridional scattering, which changes significantly during deformation (Figs 5(a–d) and 6) despite the intensity of the equatorial scattering hardly changing at all. As the sample is strained, the rubber particles (initially elongated due to processing history) become more elongated and the scattering intensity on the meridian moves to a lower angle. This can be seen in Fig. 6 for the first 10 frames of data. However, as the strain increases further, the scattering intensity moves out again, as shown for frame 20 (a total extension of 2.7 mm). This result indicates that an additional source of scattering is developing with a shorter characteristic length scale than that of the rubber particles themselves (i.e., the form factor), giving rise to the additional meridional scattering. As the strain continues to increase, the meridional scattering intensity now shifts to a lower angle, as shown in the data for frame 40 at a total extension of 5.4 mm. This shift implies that whatever is causing this scattering is increasing in size as the strain increases.

It is clear from the previous discussion that this rubber-toughened PMMA film does not craze during tensile straining. The ESEM evidence shows that the rubber particles are voiding, and these voids (whether due to cavitation of the rubber layer or local debonding at a PMMA-rubber interface) are the source of the additional scattering apparent on the meridian of the SAXS pattern. When core–shell rubber particles in a matrix are strained any cavitation or debonding which may occur is expected to occur in the first instance at the poles of the particles [20], and hence will give rise to scattering on the meridian. Computer simulation [11] has furthermore shown that when cavitation or debonding does occur at the poles, the meridional scattering increases significantly in intensity, and new strong meridional reflections also appear at higher angle. The separate identification of these new reflections may not in general be possible, unless low q values can be accessed. In our earlier work using the European synchrotron radiation facility (ESRF) this identification was possible [11], but the q range at Daresbury precludes this. However, the voids initially formed may be expected to be small, so that they contribute to the meridional scattering at comparatively large q, and hence they can be detected by their effect on the meridian. As the strain increases, the size of these voids grow, leading to the meridional scattering moving to a lower angle. This result ties in with the ESEM observation which shows not only that the population of croids increases with strain, but also their size. In the final stage of deformation, the growth of the voids ultimately leads to breakdown of the sample, as can be seen from the very big cracks in Fig. 4b. This occurs on a length scale too big to be picked up by SAXS.

It is worth noting that the internal morphology of rubber particles used in our system is different from that used by Sue [2]. The rubber particles used here have a three-layer structure with a PMMA core, while in the earlier study the rubber particles had only a two-layer structure with a rubber core. This difference in rubber particle internal morphology will also influence their voiding mechanism. While the transmission electron microscopy study by Sue revealed that the rubber particles exhibit cavitation under strain, the rubber particle system studied here seems likely to exhibit debonding [21].

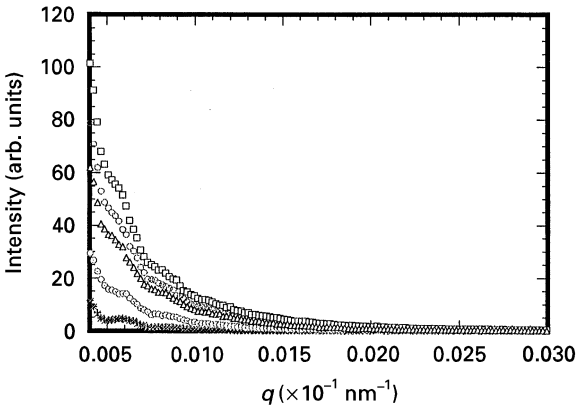

Figure 8 1-D small angle X-ray scattering curve representing the scattering from crazes in 2-D patterns for a thick sample. The key to the figure represents the number of the data frame, with extension is; (+) frame 1: 0 mm; (×) frame 10: 0.67 mm; (⊙) frame 22: 1.47 mm; (○) frame 26: 1.73 mm; (□) frame 32: 2.13 mm and (△) frame 33: 2.2 mm. $q = 4\pi \sin\theta/\lambda$.

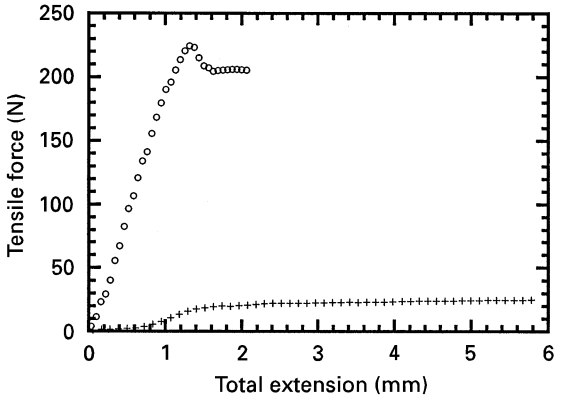

Figure 9 Load–extension curves for (+) polymer film and (○) thick samples. The strain rate for both is 0.5 mm mm^{-1}.

4.3. Comparison with thick samples

It is interesting to see that this film sample mainly exhibits a non-crazing deformation, while for a thick sample (with the same rubber particle concentration and crosslinking density, but 1200 μm thick as opposed to 100 μm), both crazing and cavitation were observed [11, 14, 17]. As shown from Fig. 8 for such a thick sample, we can see a significant change of the equatorial SAXS pattern during deformation. Initially (frames 1 to 10) the equatorial scattering does not change, indicating there is no sign of crazing. But when the extension reached 1.5 mm, there is a significant increase in the scattered intensity. This is due to crazing. The intensity of the scattering reaches a maximum at an extension of 2.13 mm, and then decreases due to the failure of craze fibrils when the sample breaks. This behaviour is in contrast to the SAXS curves for a thin sample, which as shown in Fig. 7 has a constant equatorial intensity throughout deformation. Fig. 9 compares the load–extension curves for the thin and thick samples. The fact that the thin film achieves a total extension of 6.1 mm before failure, whilst the thick sample only reaches an extension of about 2.5 mm also indicates that different deformation and fracture mechanisms govern the two types of samples, due to the different stress conditions which appertain. Such thickness effects are familiar for most types of tough polymers: the formation of crazes requires the presence of a triaxial stress, which is unlikely to be met in thin films, particularly if voiding is occurring.

5. Conclusions

Under tensile strain, rubber particles in a PMMA matrix in a thin film sample first undergo deformation, and subsequently cavitation and/or debonding. The voiding rubber particles tend to line up to form "croids", a special case of a dilatation band. The size and frequency of these croids increase with strain. Finally, larger cracks appear in the sample. The deformation and fracture mechanism of this film is seen to be different from that of a thick sample, where both crazing and non crazing deformation contribute to the plastic deformation. This study also shows that ESEM is well suited for the *in situ* study of deformation of polymer samples, and that its combination with SAXS is a powerful one.

Acknowledgements

The authors would like to thank Dr Ian Fraser from ICI plc for providing the polymer samples, Andy Eddy for assistance in using the ESEM, EPSRC for financial support and CLRC Daresbury Laboratory (UK) for access to the SAXS facility. The ESEM instrument was purchased under the Colloid Technology Programme (funded jointly by Unilever, ICI, Zeneca, Schlumberger and the DTI).

References

1. C. B. BUCKNALL, "Toughened plastics", (Applied Science, London, 1977).
2. H-J SUE, *J. Mater. Sci.* **27** (1992) 3098.
3. A. LAZZERI and C. B. BUCKNALL, *ibid* **28** (1993) 6799.
4. *Idem*, *Polym.* **36** (1995) 2895.
5. A, M. DONALD and E. J. KRAMER, *J. Mater. Sci.* **17** (1982) 1765.
6. F. HAAF, H. BREUER and J. STABENOW, *J. Macromol. Sci.* **B14** (1977) 387.
7. B. D. LAUTERWASSER and E. J. KRAMER, *Phil. Mag.* **A39** (1979) 369.
8. D. G. GILBERT and A. M. DONALD, *J. Mater. Sci.* **21** (1986) 1819.
9. G. D. DANILATOS, *Microsc. Res. Tech.* **25** (1993) 529.
10. *Idem*, *Adv. Elec. Electron Phys.* **78** (1990) 1.
11. C. HE, A. M. DONALD, M. F. BUTLER and O. DIAT, *J. Macromol Sci. Symposium*, **112** (1996) 115.
12. R. A. BUBECK, D. J. BUCKLEY, E. J. KRAMER and H. R. BROWN, *J. Mater. Sci.* **26** (1991) 6249.
13. R. E. CAMERON and A. M. DONALD, *J. Microsc.* **173** (1994) 227.
14. C. HE, A. M. DONALD and M. F. BUTLER, submitted to *Macromols.*
15. P. MEREDITH and A. M. DONALD, *J. Microsc.* **181** (1996) 23.
16. H. R. BROWN and E. J. KRAMER, *J. Macromol. Sci.-Phys.* **19B** (1981) 487.
17. C. HE, A. M. DONALD, M. F. BUTLER and O. DIAT, *Polymer* in press.

18. C. HE and A. M. DONALD, *Langmuir* **12** (1996) 6250.
19. A. M. DONALD and E. J. KRAMER, *J. Mater. Sci.* **16** (1981) 2967.
20. R. SCHIRRER, C. FOND and A. LOBBRECHT, *ibid* **31** (1996) 6409.
21. I. FRASER and R. MOORE, Private communication.

Received 9 October 1996
and accepted 1 May 1997